LETTER

doi:10.1038/nature09556

Design, function and structure of a monomeric ClC transporter

Janice L. Robertson[1], Ludmila Kolmakova-Partensky[1] & Christopher Miller[1]

Channels and transporters of the ClC family cause the transmembrane movement of inorganic anions in service of a variety of biological tasks, from the unusual—the generation of the kilowatt pulses with which electric fish stun their prey—to the quotidian—the acidification of endosomes, vacuoles and lysosomes[1]. The homodimeric architecture of ClC proteins, initially inferred from single-molecule studies of an elasmobranch Cl^- channel[2] and later confirmed by crystal structures of bacterial Cl^-/H^+ antiporters[3,4], is apparently universal. Moreover, the basic machinery that enables ion movement through these proteins—the aqueous pores for anion diffusion in the channels and the ion-coupling chambers that coordinate Cl^- and H^+ antiport in the transporters—are contained wholly within each subunit of the homodimer. The near-normal function of a bacterial ClC transporter straitjacketed by covalent cross-links across the dimer interface and the behaviour of a concatemeric human homologue argue that the transport cycle resides within each subunit and does not require rigid-body rearrangements between subunits[5,6]. However, this evidence is only inferential, and because examples are known in which quaternary rearrangements of extracellular ClC domains that contribute to dimerization modulate transport activity[7], we cannot declare as definitive a 'parallel-pathways' picture in which the homodimer consists of two single-subunit transporters operating independently. A strong prediction of such a view is that it should in principle be possible to obtain a monomeric ClC. Here we exploit the known structure of a ClC Cl^-/H^+ exchanger, ClC-ec1 from *Escherichia coli*, to design mutants that destabilize the dimer interface while preserving both the structure and the transport function of individual subunits. The results demonstrate that the ClC subunit alone is the basic functional unit for transport and that cross-subunit interaction is not required for Cl^-/H^+ exchange in ClC transporters.

To develop a strategy for generating a monomeric ClC protein, we examined the structure of ClC-ec1 (Fig. 1) for candidate residues mediating dimerization. This homologue is well suited to our purpose because its dimerization interface is almost completely membrane embedded, the large intracellular carboxy-terminal domain found in some ClC proteins being absent here. The interface is formed mainly by four helices running roughly perpendicular to the membrane to create a flat, nonpolar surface of ~1,200 $Å^2$ (Fig. 1). Most cross-subunit contacts are made by interdigitated leucine and isoleucine side chains; residues capable of forming hydrogen bonds or salt bridges are absent. The protein's phospholipid-facing residues are also nonpolar (Fig. 1), a circumstance that invites questions of how such chemically similar surfaces so faithfully choose their respective protein and lipid partners in the dimer. Such questions have motivated extensive studies of transmembrane peptide dimerization[8–10], which identified shape complementarity as an important determinant of helix packing specificity within membranes and micelles. Shape complementarity of the ClC-ec1 dimer interface is high, scoring at levels seen for protein-antibody contacts and several membrane protein oligomers (Supplementary Table 1). Accordingly, our design strategy seeks to destabilize the dimer by placing steric mismatches on the ClC subunit interface. A second element of the strategy aims at favouring the interface's exposure to the lipid bilayer. Lipid-facing surfaces of many membrane proteins are known to present amphiphilic tryptophan or tyrosine side chains to the chemically heterogeneous transition zone where the lipid acyl chains connect to the polar head groups, as seen for ClC-ec1 in Fig. 1; membrane-thermodynamic analysis of tryptophan analogues establishes that the aromatic, bifunctional character of this side chain favours its location at the phospholipid bilayer's transition zone[11].

With these considerations in mind, we adopted a 'warts-and-hooks' strategy for engineering a monomeric ClC by introducing tryptophan

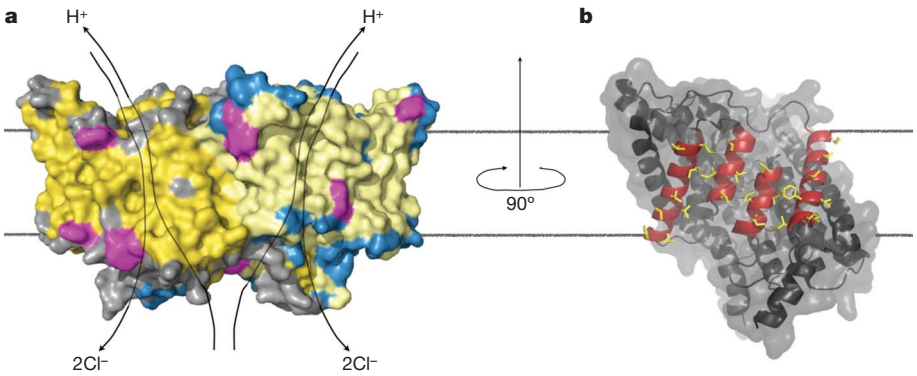

Figure 1 | Structure and dimeric interface of ClC-ec1. a, ClC-ec1 dimer (Protein Data Bank ID, 1OTS) is shown with subunits in grey and blue, with hydrophobic residues highlighted in yellow, and with tryptophan and tyrosine in magenta. The level of the membrane (extracellular side up) is indicated by black lines. Previously proposed transport pathways are shown for Cl^- and H^+. **b**, Single subunit rotated 90° to view the dimerization interface head-on. The four interface helices (residues 192–204, 215–232, 405–416 and 422–440) are shown in red and the side chains involved in cross-subunit contacts are shown in yellow.

[1]Department of Biochemistry, Howard Hughes Medical Institute, Brandeis University, Waltham, Massachusetts 02454, USA.

mutations on the subunit interface near the level of the lipid head groups. This type of substitution simultaneously offers two kinds of perturbation: steric disruption of the contact surface's shape complementarity and enhanced affinity of this surface for the lipid bilayer. We constructed eight single tryptophan substitutions for leucine or isoleucine near the extracellular and intracellular ends of the four dimerization helices (Fig. 2a). All but one of these mutants express near wild-type levels, and the oligomerization state of each was analysed in decylmaltoside micelles on a size exclusion column calibrated with a panel of membrane transport proteins[12] (Fig. 2b). The wild-type homodimer (100 kDa) elutes, as expected, at 12.8 ml, and the 50-kDa monomer is predicted to elute about 1 ml later. One mutant, Ile 422 Trp, shifts precisely to the presumed monomer position, with a minor dimer peak also apparent. Three other mutants, Ile 201 Trp, Leu 406 Trp and Leu 434 Trp, show broader, asymmetric peaks centred between dimer and monomer positions. The remaining three mutants all run as dimers (data not shown). In hopes of further stabilizing a monomer, we tested the double mutant Ile 201 Trp/Ile 422 Trp, which if dimeric would place four 'warts' within the subunit contact region, and if monomeric would offer two 'hooks' to the bilayer, one on each side of the membrane. This mutant, henceforth denoted WW, cleanly shifts to the monomer position with no observable dimer peak. The oligomeric nature of this double mutant in detergent micelles was further assessed by treatment with glutaraldehyde, a promiscuous crosslinker known quantitatively to produce covalent dimers of ClC-ec1[13], as illustrated for the wild type by SDS–polyacrylamide gel electrophoresis (Fig. 2c). In contrast, glutaraldehyde treatment fails to shift WW to the covalent-dimer position, thereby identifying it as a monomer in detergent.

To identify the oligomeric state of WW in lipid bilayers, we repeated glutaraldehyde crosslinking experiments on this protein reconstituted into liposomes. Phosphatidylcholine–phosphatidylglycerol mixtures were used here to avoid lipid-associated amino groups that would confound the glutaraldehyde reaction. We also aimed in these experiments to approximate Poisson-dilution conditions[14], wherein a low protein/lipid ratio is used so that most liposomes are protein free and any liposome containing protein carries only a single transporting unit. Under such conditions, each liposome becomes a single-molecule reaction vessel in which intramolecular crosslinking is favoured. As shown in Fig. 3a, crosslinking in liposomes recapitulates the detergent results, thereby showing that WW is also monomeric in these bilayer membranes.

The experiments above establish the WW mutant as monomeric but do not address its conformational or functional character. We therefore performed two mechanistically diagnostic ion-transport measurements in the same liposome environment as was used for the crosslinking experiments. The unitary passive Cl^- transport rate was determined in a 'Cl^- dump' experiment[14], in which liposomes with high Cl^- concentration are suspended in low-Cl^- solution in the presence of H^+ and K^+ ionophores, to prevent a pH gradient build-up and to maintain zero voltage. Under these conditions, the unitary Cl^- efflux rate of wild-type protein, measured electrochemically by the appearance of Cl^- in the external solution (Fig. 3b), is $\sim 300\ s^{-1}$; Cl^- turnover by WW is roughly half of this value ($160\ s^{-1}$), a respectable activity. Furthermore, anion specificity of transport is maintained in WW, as Cl^- efflux is fully dependent on addition of K^+ ionophore. ClC-ec1 is a coupled Cl^-/H^+ exchanger, in which a pre-established Cl^- gradient can be used to pump H^+ thermodynamically 'uphill'[15]. The WW monomer retains this defining feature of the transport

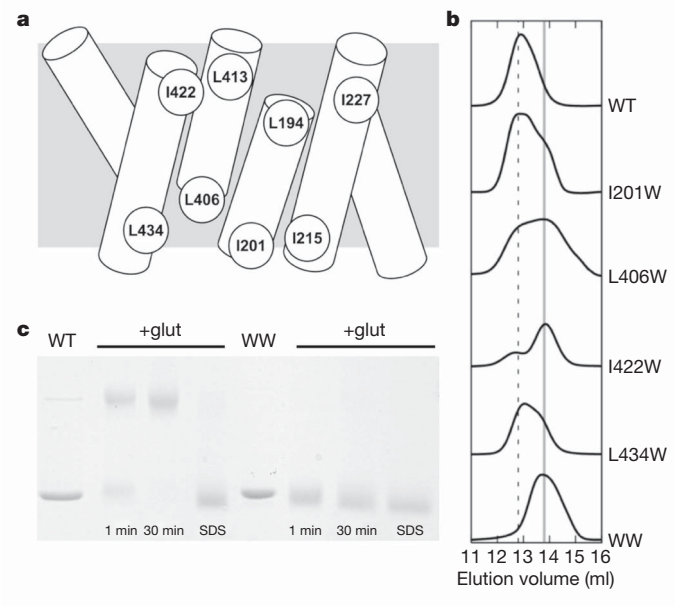

Figure 2 | Behaviour of tryptophan mutants in detergent. **a**, Schematic of the dimerization interface showing the positions of the tryptophans tested. Leu 194 Trp did not express protein. **b**, Chromatographic profiles of the various mutants on a Superdex 200 column. Vertical lines mark elution volumes for dimer (dashed) and monomer (solid). WT, wild type. **c**, 10% SDS–polyacrylamide gel electrophoresis of wild-type and WW samples, Coomassie stained. Bars indicate samples at 0.25 mg ml^{-1} treated with 0.125% glutaraldehyde, 150 mM NaCl and 50 mM Na phosphate, pH 7.0, for the indicated times in 5 mM decylmaltoside or, as a negative control, in 2% SDS. Crosslinking is nearly complete after 1 min, and no higher oligomers appear even after 30 min.

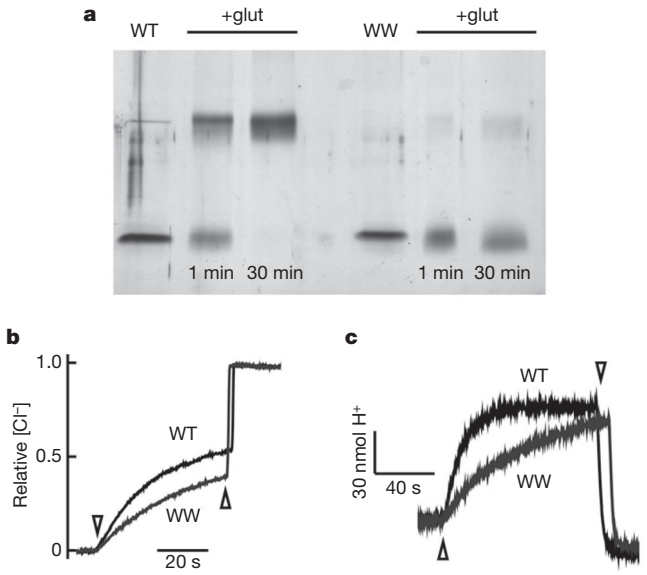

Figure 3 | Monomeric ClC mutant in phospholipid membranes. **a**, Glutaraldehyde crosslinking of wild-type ClC-ec1 and the WW mutant in liposomes. Glutaraldehyde treatment was as in Fig. 2, except that protein was incorporated into phosphatidylcholine–phosphatidylglycerol liposomes, and gel was silver stained. **b**, Passive Cl^- efflux from reconstituted liposomes for wild-type ClC-ec1 and the WW mutant. Traces show release of Cl^- from liposomes loaded with 300 mM Cl^- into the extraliposomal solution (containing 1 mM Cl^-), initiated by 0.5 μM valinomycin (downward arrowhead), normalized to the level of complete release on disrupting liposomes with 50 mM octylglucoside (upward arrowhead). Unitary turnover calculated on a per-subunit basis from the initial rate of Cl^- release[14] was $290 \pm 30\ s^{-1}$ for wild type, $160 \pm 9\ s^{-1}$ for WW (mean ± s.e.m., $N = 9$). [Cl^-], Cl^- concentration. **c**, Cl^--driven H^+ pumping against a pH gradient. Liposomes loaded with 300 mM Cl^-, pH 5.0, were suspended in 1 mM Cl^-, pH 5.2, and transport was initiated by valinomycin (upward arrowhead) and terminated by carbonyl cyanide-*p*-trifluoromethoxyphenylhydrazone (FCCP, downward arrowhead), while the pH of the suspension was recorded. Upward deflection represents uptake of H^+ into liposomes.

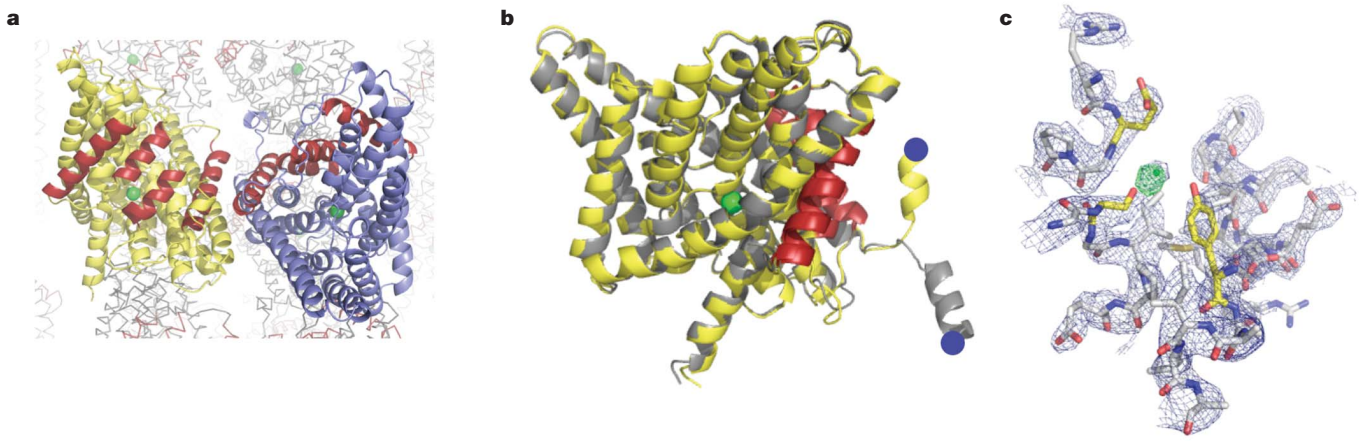

Figure 4 | Crystal structure of the WW monomer. **a**, View of two monomers in side-by-side contact, with interface helices highlighted in red, Cl^- ion highlighted in green and additional symmetry-related monomers shown in grey in the background. **b**, Backbone alignment (Cα root mean squared deviation, 0.6 Å) of the WW monomer (yellow, with interface helices in red) with a single subunit of wild-type ClC-ec1 (grey). Blue spheres indicate the N termini of the visible structures. **c**, Central anion-binding site. The $2F_o–F_c$ map (blue, 1.5σ) is shown near the central Cl^--binding site, with coordinating residues Ser 107, Glu 148 and Tyr 445 highlighted (yellow); the positive difference density calculated from a Cl^--omit map (green) shows a strong peak (3.5σ) at the position of the central Cl^- ion in the wild type. Stereo versions of panels **a** and **c** can be found in Supplementary Fig. 2.

mechanism. As shown in Fig. 3c, Cl^--loaded liposomes are suspended in low-Cl^- medium, and transport is initiated by depolarizing the liposomes with K^+ ionophore. As Cl^- flows out, H^+ enters against a pH gradient, as detected by alkalinization of the extraliposomal medium, which is swiftly reversed by addition of a proton ionophore. We established Cl^-/H^+ exchange stoichiometry from the ratio of initial flux rates (Supplementary Fig. 1): 2.0 ± 0.1 for the wild-type control, as expected from the two-to-one stoichiometry determined in *E. coli* lipids[14–16], and a similar value, 2.3 ± 0.3, for WW. The preservation of H^+-coupled Cl^- antiport in the monomeric construct directly establishes that the ClC subunit contains all essential components of the transport mechanism. The possibility remains that side-chain movements at the dimer interface in wild-type homodimer may occur during the transport cycle, as indicated convincingly by recent ^{19}F NMR experiments[17], but our results demonstrate that such movements cannot represent functionally obligatory cross-subunit interactions.

We crystallized the WW mutant, collected X-ray diffraction data to a resolution of 3.1 Å and solved the structure by molecular replacement using the wild-type subunit as search model (crystallographic statistics are shown in Supplementary Table 2). The asymmetric unit consists of a single monomer whose previously buried dimer interface is now completely exposed to detergent-containing solvent. This exposed interface is shown in Fig. 4a (also see Supplementary Fig. 2) for a symmetry-related pair of monomers, whose contacts in the unit cell arise from crystal geometry and are not seen in crystals of wild-type ClC-ec1. We consider it remarkable that the monomer's 18 membrane-embedded helices align precisely with those of the wild-type subunit in the homodimer (Fig. 4b), despite the absence of native cross-subunit interactions. Only the cytoplasmic amino-terminal helix (residues 22–30), which in the wild type engages in a domain swap with its twin subunit, veers off in a different direction to accommodate crystal packing. Moreover, most side chains projecting from the exposed subunit interface are well ordered and unperturbed from their buried positions in the wild-type dimer, except for a single tyrosine, which adopts a different rotamer to make room for one of the substituted tryptophans (Supplementary Fig. 3). Unambiguous density for the mechanistically crucial central Cl^- ion appears in the monomer at the same position as in the wild type, coordinated by the central serine and tyrosine residues (Fig. 4 and Supplementary Fig. 2); however, Cl^- density is lower in WW than in wild-type data sets of similar crystallographic quality[18], perhaps because crystallization of the monomer requires the additional presence of NO_3^-, a transported anion known to compete with Cl^- (refs 13, 19).

A perplexing clash of form and function arises from this demonstration that the isolated ClC subunit is transport competent: why then are all known ClC proteins homodimers? With the steady expansion of the membrane protein structural database, it is becoming apparent that the parallel-pathways theme discussed here for ClCs appears in many families of channels and transporters. For instance, aquaporin channels are homotetramers with a diffusion pore in each subunit[20], FNT-family formate channels are five-pore pentamers[21,22] and UT-family urea channels[23], Amt-type ammonia channels[24,25] and outer-membrane porins[26] are three-pore trimers. Among membrane transporters, a striking example is found in five phylogenetically unrelated families whose transporting subunits share a common structural fold but variously assemble as monomers, dimers or trimers[27,28]. A survey of the current literature identifies no fewer than fourteen separate families (~40% of structurally known membrane transport protein families) built on this parallel-pathway principle, with subunits held together through extended, nonpolar intramembrane contacts. We are loath to offer any suggestion for the 'meaning'—evolutionary or physiological—of this emerging structural theme; in only one case, a trimeric Na^+-coupled aspartate transporter of the EAAT superfamily[29], has parallel-pathway architecture been plausibly proposed as essential for substrate transport by the individual subunits making up the complex.

Although our warts-and-hooks design succeeded in severing the ClC dimer, we do not claim to understand the thermodynamic reasons for its success. The energetic components governing how a greasy protein surface chooses its greasy protein partner over a greasy lipid bilayer are still unparsed. Previous attempts to attack this fundamental problem of membrane protein chemistry have focused on model systems of single transmembrane helical peptides[8–10,30], and most have been quantifiable only in detergent micelles. The ClC interface introduced here may provide future opportunities to examine the molecular forces operating in transmembrane helix packing, folding and recognition in the context of a complex integral membrane protein.

METHODS SUMMARY

Expression in *E. coli*, purification and liposome reconstitution of ClC-ec1 (Swiss-Prot ID, P37019) were performed as described[14], as were Cl^- and H^+ flux assays, except that we used lipid mixtures of egg phosphatidylcholine and 1-palmitoyl, 2-oleoyl phosphatidylglycerol in a 3/1 weight ratio. Ion flux rates in these lipids are 5–10-fold lower than observed in the *E. coli* phospholipids that we customarily use. Liposomes were formed at 20 mg ml^{-1} lipid, 1 μg protein per milligram lipid by dialysis, or by centrifugation of 0.1-ml samples through 3-ml Sephadex G-50 columns. Cl^-/H^+ exchange stoichiometry was determined as the ratio of initial

transport rates[16], with Cl^- efflux and H^+ uptake recorded by means of Cl^- and H^+ electrodes using liposomes loaded with 300 mM KCl and 40 mM citrate-NaOH, pH 5.0, suspended in solutions of 1 mM KCl, 300 mM K isethionate and 2 mM citrate-NaOH, pH 5.2. For crystallography, 1 µl ClC protein (9–15 mg ml^{-1}) in 100 mM NaCl, ~40 mM decylmaltoside and 10 mM Tris-HCl, pH 7.5, was mixed with an equal volume of 100 mM $LiNO_3$, 41–45% (w/v) PEG400, 100 mM glycine-NaOH, pH 9.5, and ~10 mM 4-cyclohexyl-1-butyl-β-D-maltoside was added to the 2-µl drop. Crystals grown by vapour diffusion in sitting drop trays for 2–4 weeks at 20 °C were frozen in liquid nitrogen, and data were collected remotely at beamline 8.2.1 of the Advanced Light Source Eastern Annex, Waltham, Massachusetts. Data were processed in HKL2000. Molecular replacement was done in PHASER using residues 30–450 of a single subunit of ClC-ec1 as search model, and refinement was carried out in REFMAC5.

Received 22 June; accepted 5 October 2010.
Published online 3 November 2010.

1. Jentsch, T. J. *et al.* Physiological functions of CLC Cl^- channels gleaned from human genetic disease and mouse models. *Annu. Rev. Physiol.* **67,** 779–807 (2005).
2. Middleton, R. E., Pheasant, D. J. & Miller, C. Reconstitution of detergent-solubilized Cl^- channels and analysis by concentrative uptake of $^{36}Cl^-$ and planar lipid bilayers. *Methods* **6,** 28–36 (1994).
3. Dutzler, R. *et al.* X-ray structure of a ClC chloride channel at 3.0 Å reveals the molecular basis of anion selectivity. *Nature* **415,** 287–294 (2002).
4. Dutzler, R., Campbell, E. B. & MacKinnon, R. Gating the selectivity filter in ClC chloride channels. *Science* **300,** 108–112 (2003).
5. Nguitragool, W. & Miller, C. CLC Cl^-/H^+ transporters constrained by covalent cross-linking. *Proc. Natl Acad. Sci. USA* **104,** 20659–20665 (2007).
6. Zdebik, A. A. *et al.* Determinants of anion-proton coupling in mammalian endosomal CLC proteins. *J. Biol. Chem.* **283,** 4219–4227 (2008).
7. Bykova, E. A. *et al.* Large movement in the C terminus of CLC-0 chloride channel during slow gating. *Nature Struct. Mol. Biol.* **13,** 1115–1119 (2006).
8. Fleming, K. G., Ackerman, A. L. & Engelman, D. A. The effect of point mutations on the free energy of transmembrane α-helix dimerization. *J. Mol. Biol.* **272,** 266–275 (1997).
9. MacKenzie, K. R. & Fleming, K. G. Association energetics of membrane spanning α-helices. *Curr. Opin. Struct. Biol.* **18,** 412–419 (2008).
10. Chen, L. *et al.* Energetics of ErbB1 transmembrane domain dimerization in lipid bilayers. *Biophys. J.* **96,** 4622–4630 (2009).
11. Yau, W. M. *et al.* The preference of tryptophan for membrane interfaces. *Biochemistry* **37,** 14713–14718 (1998).
12. Fang, Y., Kolmakova-Partensky, L. & Miller, C. A bacterial arginine-agmatine exchange transporter involved in extreme acid resistance. *J. Biol. Chem.* **282,** 176–182 (2007).
13. Maduke, M., Pheasant, D. J. & Miller, C. High-level expression, functional reconstitution, and quaternary structure of a prokaryotic ClC-type chloride channel. *J. Gen. Physiol.* **114,** 713–722 (1999).
14. Walden, M. *et al.* Uncoupling and turnover in a Cl^-/H^+ exchange transporter. *J. Gen. Physiol.* **129,** 317–329 (2007).
15. Accardi, A. & Miller, C. Secondary active transport mediated by a prokaryotic homologue of ClC Cl- channels. *Nature* **427,** 803–807 (2004).
16. Miller, C. & Nguitragool, W. A provisional transport mechanism for a chloride channel-type Cl^-/H^+ exchanger. *Phil. Trans. R. Soc. B* **364,** 175–180 (2008).
17. Elvington, S. M., Liu, C. W. & Maduke, M. C. Substrate-driven conformational changes in ClC-ec1 observed by fluorine NMR. *EMBO J.* **28,** 3090–3102 (2009).
18. Accardi, A. *et al.* Synergism between halide binding and proton transport in a CLC-type exchanger. *J. Mol. Biol.* **362,** 691–699 (2006).
19. Nguitragool, W. & Miller, C. Uncoupling of a CLC Cl^-/H^+ exchange transporter by polyatomic anions. *J. Mol. Biol.* **362,** 682–690 (2006).
20. Fu, D. *et al.* Structure of a glycerol-conducting channel and the basis for its selectivity. *Science* **290,** 481–486 (2000).
21. Wang, Y. *et al.* Structure of the formate transporter FocA reveals a pentameric aquaporin-like channel. *Nature* **462,** 467–472 (2009).
22. Waight, A. B., Love, J. & Wang, D. N. Structure and mechanism of a pentameric formate channel. *Nature Struct. Mol. Biol.* **17,** 31–37 (2010).
23. Levin, E. J., Quick, M. & Zhou, M. Crystal structure of a bacterial homologue of the kidney urea transporter. *Nature* **462,** 757–761 (2009).
24. Khademi, S. *et al.* Mechanism of ammonia transport by Amt/MEP/Rh: structure of AmtB at 1.35 Å. *Science* **305,** 1587–1594 (2004).
25. Zheng, L. *et al.* The mechanism of ammonia transport based on the crystal structure of AmtB of *Escherichia coli*. *Proc. Natl Acad. Sci. USA* **101,** 17090–17095 (2004).
26. Cowan, S. W. *et al.* Crystal structures explain functional properties of two *E. coli* porins. *Nature* **358,** 727–733 (1992).
27. Shaffer, P. L. *et al.* Structure and mechanism of a Na^+-independent amino acid transporter. *Science* **325,** 1010–1014 (2009).
28. Theobald, D. L. & Miller, C. Membrane transport proteins: surprises in structural sameness. *Nature Struct. Mol. Biol.* **17,** 2–3 (2010).
29. Reyes, N., Ginter, C. & Boudker, O. Transport mechanism of a bacterial homologue of glutamate transporters. *Nature* **462,** 880–885 (2009).
30. Metcalf, D. G. *et al.* Multiple approaches converge on the structure of the integrin αIIb/β3 transmembrane heterodimer. *J. Mol. Biol.* **392,** 1087–1101 (2009).

Supplementary Information is linked to the online version of the paper at www.nature.com/nature.

Acknowledgements We are grateful to the scientists at beamline 8.2.1 of the Advanced Light Source, Lawrence Berkeley Laboratory, for much help and advice, to H. Jayaram for help with refinement, and to R. Sah and D. Theobald for comments on the manuscript.

Author Contributions Experiments were designed by J.L.R. and C.M. and carried out by J.L.R. and L.K.-P., and the manuscript was written by all authors.

Author Information The atomic coordinates and structure factors of the WW (Ile 201 Trp/Ile 422 Trp) monomer have been deposited in the Protein Data Bank under accession code 3NMO. Reprints and permissions information is available at www.nature.com/reprints. The authors declare no competing financial interests. Readers are welcome to comment on the online version of this article at www.nature.com/nature. Correspondence and requests for materials should be addressed to C.M. (cmiller@brandeis.edu).